Selective Demodulation Scheme Based on Log-Likelihood Ratio Threshold

Yuheng Huang[1], *Yan Dong[1], *Minho Jo[2] and Yingzhuang Liu[1]
[1]Department of Electronics and Information Engineering, Huazhong University of Science &Technology, China
[e-mail : huangyuheng@smail.hust.edu.cn, dongyan@mail.hust.edu.cn, liuyz@mail.hust.edu.cn]
[2]Department of Computer and Communication, Korea University, Seoul, South Korea
[e-mail: minhojo@korea.ac.kr]
*Corresponding author: Yan Dong, Minho Jo

Received January 6, 2012; revised March 5, 2013; accepted March 29, 2013; published April 30, 2013

Abstract

This paper aims at designing a selective demodulation scheme based on Log-likelihood Ratio threshold (SDLT) instead of the conventional adaptive demodulation (ADM) scheme, by using rateless codes. The major difference is that the Log-likelihood ratio (LLR) threshold is identified as a key factor to control the demodulation rate, while the ADM uses decision region set (DRS) to adjust the bit rate. In the 16-QAM SDLT scheme, we deduce the decision regions over an additive white Gaussian channel, corresponding to the variation of LLR threshold and channel states. We also derived the equations to calculate demodulation rate and bit error rate (BER), which could be proven by simulation results. We present an adaptation strategy for SDLT, and compare it with ADM and adaptive modulation (AM). The simulation results show that our scheme not only significantly outperforms the ADM in terms of BER, but also achieves a performance as good as the AM scheme. Moreover, the proposed scheme can support much more rate patterns over a wide range of channel states.

Keywords: Selective demodulation, log-likelihood ratio, decision region, rateless codes

This work was supported by "the MSRA-National Natural Science Foundation of China joint funding (No.60933012)", "the MSRA-National Natural Science Foundation of China joint funding (No.60933012)", "the National Research Foundation of Korea grant funded by the Korea government (MEST) (No. 2011-0009454)" and "the China-Korea Joint Research Project on the Next Generation Green Wireless Cellular Networks, China Ministry of Science & Technology (No.2012DFG12250)".

http://dx.doi.org/10.3837/tiis.2013.04.009

1. Introduction

The rate adaptive solutions have been widely researched to improve the transmission efficiency and reliability in wireless communication [1]. Depending on the location of the rate adjustment, these solutions can be categorized into either sender rate adaptation or receiver rate adaptation. Two popular sender rate adaptation schemes are AM and adaptive modulation coding (AMC). In the classical AM system [2][3], the transmitter dynamically adjusts the modulation lever according to the channel state information (CSI). In contrast to AM systems, the AMC systems support more transmission modes which are implemented by combining different modulation and coding schemes, as in [4][5].

Whether AMC or AM, these schemes present several difficulties. All sender rate adaptation systems work with the assumption that the transmitter needs to know the relatively accurate knowledge of the channel. Typically, the transmitter obtains knowledge of the channel state from the receiver by means of a feedback path, which may consume a significant amount of overhead, especially if CSI changes rapidly. Furthermore, it is difficult to acquire the channel state at the transmitter in several scenarios.

The receiver rate adaptation schemes, such as the incremental redundancy (IR) scheme [6][7], have been widely studied to tackle those issues mentioned above. IR schemes (specifically type-II hybrid ARQ schemes) avoid the requirement for channel feedback to the transmitter, but instead require a second-layer ARQ protocol scheme to operate. An additional complication of IR is that the decoding procedure is repeated after each sub-packet is received to check for successful transmission, thus, essentially wastes resources each time the decoding scheme fails. Another problem is the potentially large buffer size, which results in the low utilization efficiency under poor channel conditions. Actually, buffer size was a significant parameter and cannot be neglected in many wireless communication scenarios [8]. The ADM scheme using rateless codes and the controlled soft demodulation scheme [9] are proposed to avoid these pitfalls. In the ADM system [10][11], the transmitter encodes the data packet with a rateless code such as Raptor code and modulates it with one of the standard modulation schemes, while the receiver demodulates the bits at a non-fixed rate by using DRS. The primary reason to use a rateless code for ADM is that it could allow the recovery of message which was dropped by the DRS. Compared with the IR system, the ADM scheme has a simple decoding mechanism and a fixed buffer size. It also overcomes the limitation of the IR scheme, since a second layer of ARQ is not needed. Due to these advantages, ADM has been considered as a representative solution of the receiver rate adaptation schemes. However, only a few rate patterns are available in the ADM, since the number of patterns for DRS is limited by the order of modulation. It is clear that the shortage in patterns restricts the developmen of ADM.

In this paper, we propose a selective demodulation based on LLR threshold (SDLT) instead of the conventional ADM system. Essentially, the proposed SDLT scheme has the advantages of ADM, since SDLT has similar encoding and decoding algorithm as the ADM. The main difference is that our demodulated bit selection is implemented by the LLR threshold instead of DRS. In SDLT scheme, the receiver only demodulates those bits with LLR exceeding a preset threshold, and treats the non-demodulated bits as erasures. Thus, the LLR threshold is identified as a key factor to control the demodulation rate. In order to illustrate the accuracy and validity of the proposed SDLT scheme, we focus on the deleting region in in constellation, and analyse the decision regions under a different set of parameters. We also derive the

theoretical expressions of demodulation rate and BER, and this derivation is proved by simulation results. The dynamic LLR threshold criterion for selective demodulation is presented, where the demodulator dynamically adjusts the threshold according to the observed channel state information (CSI) at the receiver. Compared with the ADM, our scheme increases the probability of discarding incorrect bits, and offers remarkable increases in BER performance. Moreover, SDLT supports a great many of transmission patterns, since the threshold adjustment can be implemented easily.

The remainder of the paper is organized as follows. Section 2 contains an overview of Raptor code and LLR calculation, along with the system model. The decision regions for SDLT are proposed in section 3, where the derivation process is also addressed in detail. In section 4, we derived the expression of demodulation rate and BER, by using the proposed decision region. Dynamic adaptation of LLR threshold in SDLT are proposed in Section 5, followed by the simulation results. Finally, Section 6 provides a brief summary of the article.

2. System Model

Since Raptor codes and the LLR calculuation are integral parts of our scheme, we briefly discuss them here before presenting the system model.

2.1 Raptor Codes

The primary reason to use the erasure codes in our scheme is that it could allow recovery of the message which was dropped in selective demodulation. A remarkable example of erasure codes is the LT codes [12], which is also an important ratless code. LT codes can generate and spray infinitely long encoded message and terminate only when the receiver sends the acknowledgement. The Raptor code [13] extends these ideas to reduce encoding and decoding complexity, which contains two different codes: Low Density Parity Check code (LDPC) and LT code. If we view a code as a mapping from one set of bits to another, the Raptor codes can be described by

$$Raptor(x) = LT(LDPC(x))$$

where x represents a block of bits. To code a block of bits using Raptor code, it needs first encode the block using the LDPC code. The resulting block is then coded using LT code, and the process of the decoding is reversed.

Although rateless codes were originally designed for binary erasure channels (BEC), they can achieve error correction with belief propagation (BP) decoding over the AWGN channel and the fading channels[14][15][16].

2.2 LLR Calculation

In a soft-input decoder, the channel demodulator output is generally de-mapped and used as an input value for the decoder. Let $b_{i,k}$ represent the encoded information bit sequence with the Raptor code, where i is the bit index in a modulated symbol and k is the symbol index in the symbol sequence S_k. The optimum hard decision on $b_{i,k}$ is given by the rule:

$$b_{i,k} = \beta \quad if \quad P[b_{i,k} = \beta | r_k] > P[b_{i,k} = (1-\beta) | r_k] \tag{1}$$

Set $\beta = 0$, then (1) can be written as:

$$b_{i,k}=0 \quad if \quad \ln\frac{P[b_{i,k}=0|r_k]}{P[b_{i,k}=1|r_k]}>0 \tag{2}$$

where r_k represents the received symbol sequence.

Assuming each symbol has equal transmission probability, the LLR of $b_{i,k}$ can be expressed as:

$$LLR(b_{i,k}|r_k)=\ln\frac{P[b_{i,k}=0|r_k]}{P[b_{i,k}=1|r_k]} \tag{3}$$

Clearly, the absolute value of LLR indicate the decision reliability of the $b_{i,k}$, since LLR is a ratio of probabilities.

2.3 System Model

The system is described as follows. To send a message of m-bits, the first step is that the transmitter encodes the information using the Raptor code, which can produce a continuous variable-length encoded bit stream. After pre-encoding, the bit stream is modulated with Gray-mapped 16-QAM and transmitted over an AWGN channel. The signal constellation is shown in **Fig. 1**. As S_k is the transmitted symbol sequence, the received symbol sequence can be described as $r_k=S_k+n=r_{I,k}+jr_{Q,k}$, where $n=n_I+jn_Q$. n_I and n_Q are independent, additive white complex noise Gaussian processes with zero mean and variance $\sigma^2=N_0/2$.

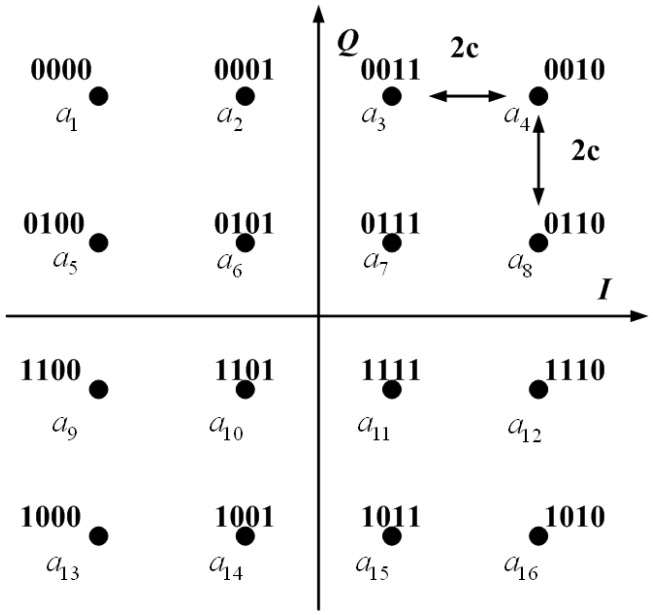

Fig. 1. 16-QAM constellation using Gray mapping. The distance between nearest neighbors is 2c

The process of SDLT is given briefly below.

(1)Based on the CSI observed by the receiver and the desired BER, the receiver selects the appropriate LLR threshold to operate selective demodulation.

(2)The receiver computes the LLR of the received bits, and compares these LLR to the preset threshold. The bits with LLR exceeding the threshold would be demodulated and bits with LLR below the threshold would be dropped as being too unreliable. The demodulated bits

are collected in a buffer, waitting to be processed.

(3)Once the buffer successfully collected any $(1+\varepsilon)m$ bits, the receiver can use BP decoding algorithm to recover the original m bits, regardless of the erasure pattern introduced by selection.

3. Decision Region of SDLT

3.1 LLR Approximate Calculation for 16QAM With Gray Mapping

In this section we compute the bit LLR for 16-QAM signal. The transmitted symbol S_k $S_k = S_{I,k} + jS_{Q,k}$ can be described as $M(b_{1,k}, b_{2,k}, b_{3,k}, b_{4,k})$, due to the mapping rule of 16QAM. Let $A_i^0 = \{\alpha_{i,1}^0, \cdots, \alpha_{i,N_0}^0\}$ represent the set of constellation points for $b_{i,k} = 0$, where there are $N_{\{0\}}$ constellation points with $b_{i,k} = 0$. Similarly, let $A_i^1 = \{\alpha_{i,1}^1, \cdots, \alpha_{i,N_1}^1\}$ be the set of points where $b_{i,k} = 1$, and there are $N_{\{1\}}$ constellation points with $b_{i,k} = 1$. Then (3) can be described as:

$$LLR(b_{i,k} \mid r_k) = \ln \frac{\sum_{\alpha \in A_i^1} P[b_{i,k} = 0 \mid r_k]}{\sum_{\alpha \in A_i^0} P[b_{i,k} = 1 \mid r_k]} \tag{4}$$

By applying Bayes rule and assuming that the transmitted symbols are equally distributed:

$$LLR(b_{ik} \mid r_k) = \ln \frac{\sum_{j=1}^{N_{\{0\}}} \frac{1}{\pi N_0} \exp\left(-\frac{\left| r_k - \alpha_{i,j}^0 \right|^2}{N_0} \right)}{\sum_{j=1}^{N_{\{1\}}} \frac{1}{\pi N_0} \exp\left(-\frac{\left| r_k - \alpha_{i,j}^1 \right|^2}{N_0} \right)} \tag{5}$$

The log-sum approximation can be used to simplify the exponential term in (5), similar to the method used in [17]. Let the energy of the shaping pulse be normalized to 1 , then 2c is the distance between nearest neighbors in constellation. We have the follow expression of LLR:

$$\left| LLR(b_{1,k}) \right| \approx \begin{cases} \frac{8}{N_0}(\left| r_{Q,k} \right| - c), & \left| r_{Q,k} \right| > 2c \\ \frac{4}{N_0} \left| r_{Q,k} \right|, & \left| r_{Q,k} \right| \le 2c \end{cases} \tag{6}$$

$$\left| LLR(b_{2,k}) \right| \approx \begin{cases} \frac{4}{N_0}(\left| r_{Q,k} \right| - 2c), & \left| r_{Q,k} \right| > 2c \\ \frac{-4}{N_0}(\left| r_{Q,k} \right| - 2c), & \left| r_{Q,k} \right| \le 2c \end{cases} \tag{7}$$

$$\left|LLR(b_{3,k})\right| \approx \begin{cases} \frac{8}{N_0}(\left|r_{I,k}\right| - c), & \left|r_{I,k}\right| > 2c \\ \frac{4}{N_0}\left|r_{I,k}\right|, & \left|r_{I,k}\right| \le 2c \end{cases} \tag{8}$$

$$\left|LLR(b_{4,k})\right| \approx \begin{cases} \frac{4}{N_0}(\left|r_{I,k}\right| - 2c), & \left|r_{I,k}\right| > 2c \\ \frac{-4}{N_0}(\left|r_{I,k}\right| - 2c), & \left|r_{I,k}\right| \le 2c \end{cases} \tag{9}$$

These approximations are very close to the true LLR for high-to-moderate SNR values. By using (6)~(9), we can calculate the LLR by $r_{I,k}$ and $r_{Q,k}$, where $r_{I,k}$ is the horizontal component of r_k and $r_{Q,k}$ is the normal component of r_k.

3.2 Decision Region of SDLT

Define T as a LLR threhold in SDLT scheme. The bits whose absolute value of LLR are smaller than T ($\left|LLR(b_{i,k}\left|r_k\right.)\right| < T$) are treated as non-demodulated bits and will be discarded. As shown in **Fig. 2**, the LLR threhold value T is drawn as the horizontal line, the abosulate LLR for $b_{1,k}$ is plotted with solid line, and the abosulate LLR for $b_{2,k}$ is plotted with the dash line.

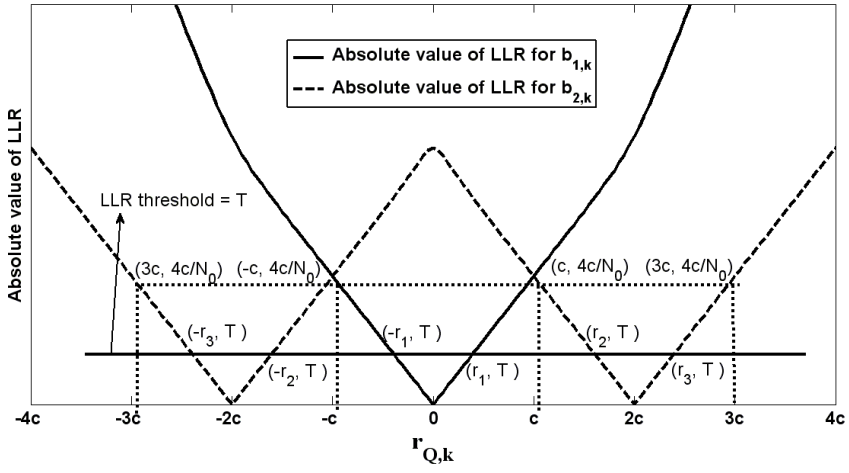

Fig. 2. The absoluate value LLR for $b_{1,k}$ and $b_{2,k}$

Through (4) and (5), we can reach a conclution that

$$\left|LLR(b_{1,k}\left|r_{Q,k}\right.=\pm c)\right| = \left|LLR(b_{2,k}\left|r_{Q,k}\right.=\pm c)\right| = \left|LLR(b_{2,k}\left|r_{Q,k}\right.=\pm 3c)\right| = \frac{4c}{N_0}$$

In order to simplify the discussion, the LLR threhold value is constrained by $0 < T \le 4c/N_0$. We begin by considering the six intersections between the horizontal line and the two curves of LLR, located at (r_1,T), $(-r_1,T)$, (r_2,T), $(-r_2,T)$, (r_3,T) and $(-r_3,T)$, where

$0 < r_1 < c < r_2 < 2c < r_3 < 3c$. Let $L_1 : \{-r_1 < r_{Q,k} < r_1\}$ be the region for deleting $b_{1,k}$ in constellation, and $L_2 : \{(-r_2 < r_{Q,k} < r_2) \bigcup (-r_3 < r_{Q,k} < r_3)\}$ be the region for deleting $b_{2,k}$. It is a relatively simple task to calculate L_1 and L_2 if we know the value of the LLR threshold, since r_1, r_2 and r_3 can be obtained by the equation (6)~(7). This can be written as

$$L_1 : \left\{ -\frac{N_0 T}{4} c < r_{Q,k} < \frac{N_0 T}{4} c \right\} \tag{10}$$

$$L_2 : \left\{ (-(2c - \frac{N_0 T}{4}) < r_{Q,k} < (2c - \frac{N_0 T}{4})) \bigcup (-(2c + \frac{N_0 T}{4}) < r_{Q,k} < (2c + \frac{N_0 T}{4})) \right\} \tag{11}$$

Define L_3 as the region for deleting $b_{3,k}$, and L_4 as the region for deleting $b_{4,k}$, L_3 and L_4 can be obtained by expressions (8)~(9).

$$L_3 : \left\{ -\frac{N_0 T}{4} c < r_{I,k} < \frac{N_0 T}{4} c \right\} \tag{12}$$

$$L_4 : \left\{ (-(2c - \frac{N_0 T}{4}) < r_{I,k} < (2c - \frac{N_0 T}{4})) \bigcup (-(2c + \frac{N_0 T}{4}) < r_{I,k} < (2c + \frac{N_0 T}{4})) \right\} \tag{13}$$

By using the expressions of deleting regions in (10)~(13), we can construct the decision region of SDLT under the contraints $0 < T \le 4c/N_0$. As shown in **Fig. 3**, this decision region is clearly very different from the standard decision regions of 16QAM. The constellation is divided into several minimal subregions.The bits labelled as '?' in each subregions means they have been dropped in the process of demodulation. Deletion of these unreliable bits will not result in decision errors, since the dropped bits could be recovered in the SDLT scheme. This also means that SDLT would result in a decrease in decision error.

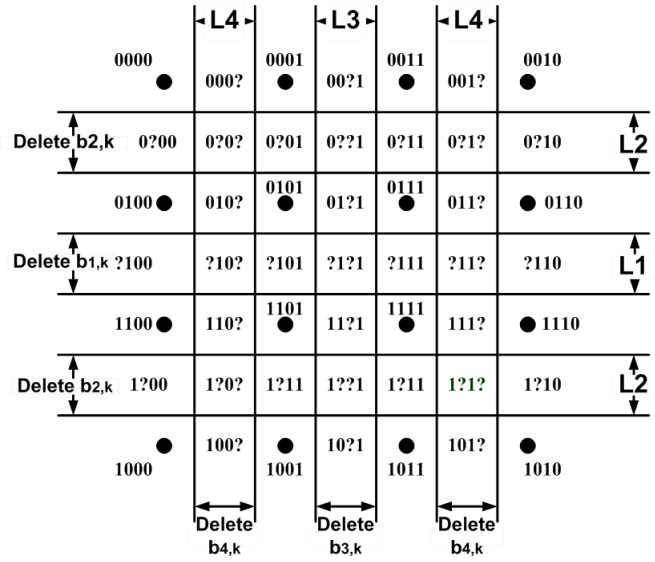

Fig. 3. The decision region of SDLT with constraints $0 < T \le 4c/N_0$

Expressions (10)~(13) also show that the deleting region tend to vary with LLR threshold and the CSI information. In particular, the deleting region increase with T if signal noise ratio

(SNR) remains unchaged. This also means that the decision region of SDLT is determined by the LLR threshold and the SNR. We analyzed the varying characteristics of the decision region, and the main results are summarized as follows: for 16-QAM Graymapped signal, no matter how the T and SNR changes, there are only four states for the decision region. In each state, T and SNR satisfy the corresponding restrict terms. All four states and their corresponding restrict terms are shown in **Fig. 3**~**Fig. 6**.

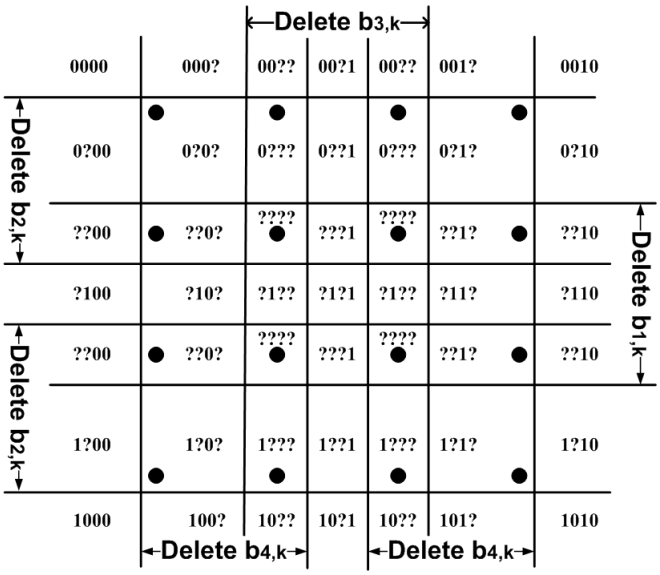

Fig. 4. The decision region of SDLT with constraints $4c/N_0 < T \le 8c/N_0$

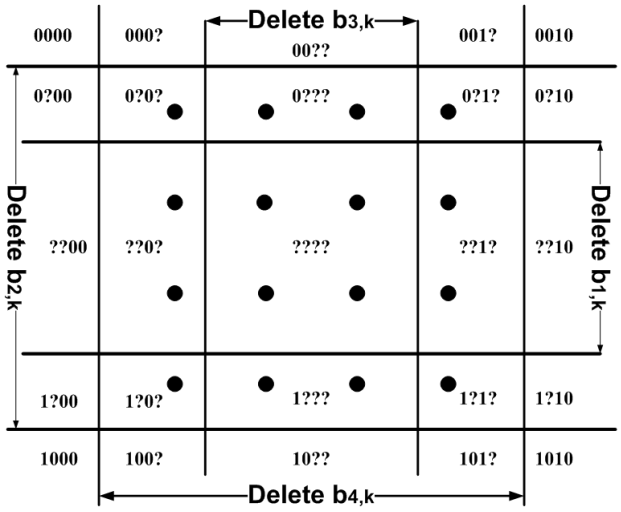

Fig. 5. The decision region of SDLT with constraints $8c/N_0 < T \le 16c/N_0$

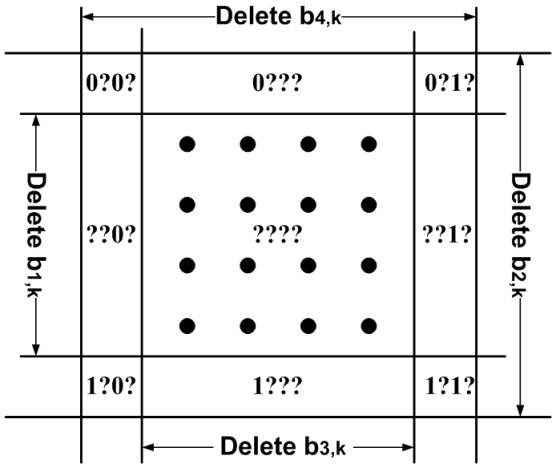

Fig. 6. The decision region of SDLT with constraints $T > 16c/N_0$

The essential difference between these four states is the location and the extent of the deleting region. To verify the derivation of the decision region, we simulate selective demodulation with different LLR threholds , and plot the position of each deleted bits. The results show that the decision regions shown in **Fig. 3**~**Fig. 6** correspond precisely to the statistics results. Actually, we can obtain the decision region accurately if T and SNR are known, by the above-mentioned restrict terms.

4. The Performance of SDLT

The decision region derived in Section 3, which allow for the simple implementation of this scheme, can be used to calculate the transmission rate and theoretical BER performance.

4.1 Transmission Rate

In the SDLT scheme, the transmission rate can be described as the demodulation rate. We define h as the proportion of the demodulated bits to the received bits in the m-bits packet. Thus the transmission rate of SDLT can be described as h-demodulation-proportion (h-DP). We consider h as the important parameter to describle the transmission rate, and the method to calculate h is described below.

We focus on the decision region shown in **Fig. 3**, where $0 < T \le 4c/N_0$. It is clear that the h-DP of each minimal subregion is determined by the number of the deleted bits. For the decision region in **Fig. 3**, if any received symbols r_k lie in the subregion labeled as "010?", the demodulator deletes $b_{4,k}$ and works at 75%-DP. We can also see that the subregion labeled as "0??1" works at 50%-DP and the subregion labeled as "0111" works at 100%-DP. Let S_1 represent the sum of the minimal subregions which work at 100%-DP. Similarly, let S_2 represent the sum of the minimal subregions which work at 75%-DP, and let S_3 represent the sum of the minimal subregions which work at 50%-DP. Thus, h for the decision region will be a weighted average of these three regions, where the weights are given by the probality that the received symbol lies in each region. This can be written as:

$$\bar{h} = P(r_k \in S_1) + 0.75 \times P(r_k \in S_2) + 0.5 \times P(r_k \in S_3) \tag{14}$$

Where $\sum_{i=1}^{3} P(r_k \in S_i) = 1$.

To calculate h-DP for the decision region, we first consider one of the transmission symbols for 16-QAM, such as a_6. As shown in **Fig. 4**, a_6 is one of the inner point of the constellation (located at $-c + jc$). All of these inner points work at the same h-DP, due to the symmetry of decision region. Let β_6 be the received symbol for a_6 over an AWGN channel, and h-DP for a_6 can be described as:

$$h_{a_6} = P(\beta_6 \in S_1) + 0.75 \times P(\beta_6 \in S_2) + 0.50 \times P(\beta_6 \in S_3) \tag{15}$$

Define P_1 as the probability of deleting $b_{1,k}$, and P_2 as the probability of deleting $b_{2,k}$. Since the the horizontal noise n_1 and the vertical noise n_2 are independent Gaussian random variables with variance σ, we can calculate P_1 by:

$$P_1 = \mathrm{P}(delete\ b_{1,k} \,|\, a_6) = \mathrm{P}((-\infty < n_1 < +\infty) \bigcap (-(1+r_1)c < n_2 < -(1-r_1)c)) \tag{16}$$

Since $Q(x)$ is the area under the tail of the Gaussian distribution $Q(x) = \int_x^{\infty} \exp(-t^2/2)\sqrt{2\pi}dt$, (16) can be expressed as:

$$P_1 = Q((1-r_1)\frac{c}{\sigma}) - Q((1+r_1)\frac{c}{\sigma}) = Q((1-r_1)\sqrt{\frac{E_s}{5N_0}}) - Q((1+r_1)\sqrt{\frac{E_s}{5N_0}}) \tag{17}$$

Where E_s is average transmission power per symbol for 16QAM ($E_s = 10c^2$). The probability of deleting $b_{2,k}$ can be writen as:

$$P_2 = Q((r_2-1)\sqrt{\frac{E_s}{5N_0}}) - Q((r_3-1)\sqrt{\frac{E_s}{5N_0}}) + Q((r_2+1)\sqrt{\frac{E_s}{5N_0}}) - Q((r_3+1)\sqrt{\frac{E_s}{5N_0}}) \tag{18}$$

Define P_3 as the probability of deleting $b_{3,k}$, and P_4 as the probability of deleting $b_{4,k}$, due to symmetry, $P_1 = P_3$, $P_2 = P_4$, the probability that β_6 lies in the three regions (S_1, S_2 and S_3) can be derived from the decision region shown in **Fig. 3**

$$P(\beta_6 \in S_1) = 1 - 2(P_1 + P_2) + (P_1 + P_2)^2 \tag{19}$$

$$P(\beta_6 \in S_2) = 2(P_1 + P_2) - 2(P_1 + P_2)^2 \tag{20}$$

$$P(\beta_6 \in S_3) = (P_1 + P_2)^2 \tag{21}$$

(14), (19), (20) and (21) can be used to obtain h-DP for a_6:

$$\begin{aligned} h_{a_6} &= 1 - 0.5[Q((1-r_1)\frac{c}{\sigma}) - Q((1+r_1)\frac{c}{\sigma}) + Q((r_2-1)\frac{c}{\sigma}) - Q((r_3-1)\frac{c}{\sigma}) \\ &+ Q((r_2+1)\frac{c}{\sigma}) - Q((r_3+1)\frac{c}{\sigma})] \end{aligned} \tag{22}$$

We can use the same method to calculate h-DP for the eight points on the sides and the four points in the corners. Since the transmitted symbols are equally distributed, the

demodulation ratio for the decision region shown in **Fig. 3** can be expressed as:

$$h = \sum_{i=1}^{16} h_{a_i} / 16 \tag{23}$$

The h-DP for the decision regions shown in **Fig. 4**~**Fig. 6** can be computed using a derivation similar to the one above. The validity and accuracy of SDLT are assessed by comparing the derivation results and the simulation results. As shown in **Fig. 7**, these theoretical calculation for h-DP with different LLR threshold are very tight to the simulation results, which confirm our theoretical analysis is valid. Most important, we proved that the demodulation rate can be precisely controlled by LLR threshold, if the SNR is fixed.

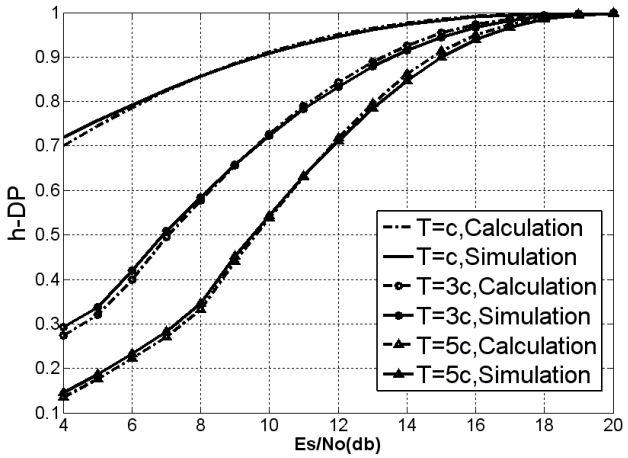

Fig. 7. h-DP for $T = c$, $T = 3c$, $T = 5c$

4.1 Bit Error Probability

To complete our analysis of SDLT, we would like to consider the BER with different LLR thresholds. The computation method is similar to the method for computing the BER of 16-QAM using standard decision regions. More attention should be paid to the concept of BER for SDLT. The BER for SDLT indicates the error probability of the demodulated bits, not of the erasures, since the erasures (labeled as "?") do not result in errors.

We begin by computing the probability of symbol error for the decision region shown in **Fig. 3**. To compute the symbol error, we begin by considering the four inner points of the constellation (located at $c + jc$, $-c + jc$, $c - jc$, $-c - jc$). We need consider only one of them, such as a_7, since all of these points have the same symbol error by symmetry. As shown in **Fig. 3**, there are eight subregions surrounding the region labeled "0111". For a_7, the symbol decision error will not occur if the received symbol lands in any of these eight subregions. Thus, we can write

$$\mathrm{P}_{SDLT}(correct \mid a_7) = \mathrm{P}((-(1+r_1)c < n_1 < (r_3 - 1)c) \bigcap (-(1+r_1)c < n_2 < (r_3 - 1)c)) \tag{24}$$

It is then straightforward to show that

$$\begin{aligned} \mathrm{P}(error|a_7) &= 2Q[(1+r_1)\sqrt{\frac{1}{5}(\frac{E_s}{N_0})}) + 2Q((r_3-1)\sqrt{\frac{1}{5}(\frac{E_s}{N_0})}] \\ &-[Q((1+r_1)\sqrt{\frac{1}{5}(\frac{E_s}{N_0})}) + Q((r_3-1)\sqrt{\frac{1}{5}(\frac{E_s}{N_0})})]^2 \end{aligned} \tag{25}$$

The following analysis can illustrate the improvement in BER for SDLT. For the standard 16QAM decision region, symbol decision error of a_7 occurs if the noise exceed c. It is given by $\mathrm{P}_{16-QAM}(correct|a_7) = \mathrm{P}((-c < n_1 < c) \bigcap (-c < n_2 < c))$. Compare this expression with (24), we can find that

$$\mathrm{P}_{16-QAM}(correct|a_7) < \mathrm{P}_{SDLT}(correct|a_7) \tag{26}$$

The expression (25) fully demostrates the BER improvement for SDLT.

The symbol error for the eight points on the sides and the four points in the corners of the 16-QAM constellation can be computed using a similar technique to the above. Aggregating result so far, we find that the symbol error for SDLT is given by

$$P_{SER,SDLT} = \sum_{i}^{16} \frac{\mathrm{P}(error|a_i)}{16} \tag{27}$$

For Gray mapped 16QAM, when symbol errors occur, the most likely symbol errors are the ones that result in only one bit error (since the nearest surrounding decision regions differ by only one bit. Thus, we can use $P_{SER,16-QAM} = 4P_{BER,16-QAM}$. For the SDLT scheme, let $4h$ as the the average number of demodulated bit per symbol, since h is the average demodulation ratio. Thus, we can approximate the bit error using $P_{SER,SDLT} = 4h \times P_{BER,SDLT}$. The BER performance with different LLR thresholds for the SDLT scheme is shown in **Fig. 8**. We find that these estimates for BER are are very close to the simulation results, and the result also proves that our analysis is valid and accurate. The result also show that the higher threhold, the better the BER performance.

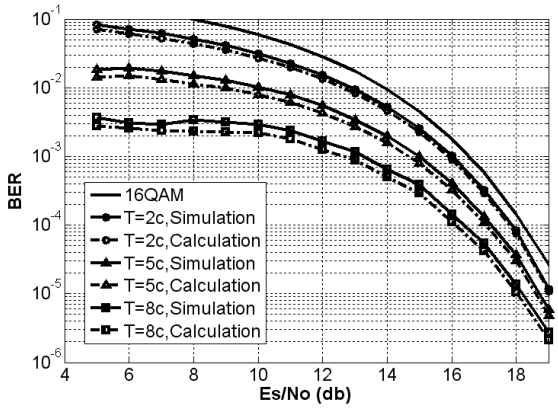

Fig. 8. BER performance for $T = c$, $T = 2c$, $T = 5c$, $T = 8c$

To satisefy the taget BER under a CSI, we can calculate a LLR threshold to make the system work at appropriate $h - DP$, by using the research result in this section.

5. Simulation Result

5.1 LLR Threshold Dynamic Adaptation

In order to maintain the demodulator working at $h-DP$, the receiver should adjust the LLR threshold adaptively according to the CSI. During a favorable channel instant, the system works at full-rate so that the receiver demodulates all the bits and $100\%-DP$ is maintained. Under a poor channel condition, a lower h would be applied and only the bits most likely to be correct would be collected in the buffer, thus decreasing the error rate at the cost of a reduced data rate. **Fig. 9** shows the normalization values of LLR threshold to achieve different $h-DP$. Most important, we proved that the demodulation rate can be precisely controlled by LLR threshold, if the SNR is fixed.

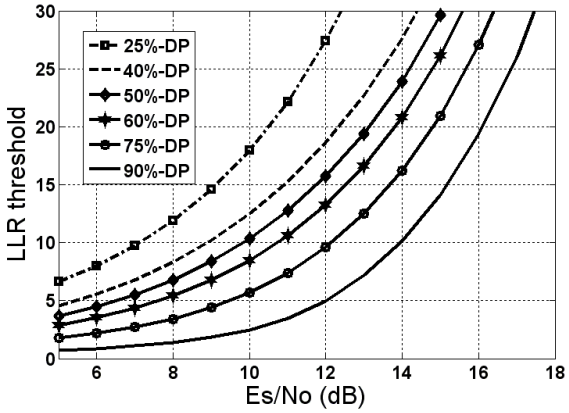

Fig. 9. Dynamic LLR threshold for $h-DP$, c=1

We demonstrate the effectiveness of our scheme, comparing with the ADM and AM schemes. The rate patterns of the ADM scheme are introduced in [10], including 16QAM, 3DRS and 2DRS. The AM system in this paper is composed of 16-QAM, 8-QAM, QPSK and BPSK . In addition, four patterns are adopted in our scheme, including 16-QAM (100%-DP), 75%-DP, 50%-DP and 25%-DP, corresponding to the ADM and AM system. The parameters of these three schemes are introduced in **Table 1**. As shown in **Table 1**, our scheme supports more rate patterns than the other two schemes.

Table 1. Parameters of different schemes

	SDLT	AM	ADM	Rate(un-coded) (bits/sec/Hz)
Mode 1 full rate	16-QAM	16-QAM	16-QAM	4
Mode 2	75%-DP	8-QAM	3-DRS	3
Mode 3	50%-DP	QPSK	2-DRS	2
Mode 4	25%-DP	BPSK	none	1
Mode n	h-DP	none	none	4*h*

We compare the BER performance of SDLT based on dynamic adaptation LLR threshold with that of ADM and AM. The BER performance for these uncoded schemes are shown in **Fig. 10**. Clearly, our scheme is superior to the ADM. This is beacause the selection in SDLT

scheme is implemented by evaluating all bits in the data packet instead of by symbol. Therefore, the probability of discarding incorrect bits will increase, resulting in BER performance improvement. This also indicates that even if the channel condition changes rapidly, SDLT system can keep the same BER performance by adjusting demodulation rate while the transmitter keeps the same modulation and coding rate.

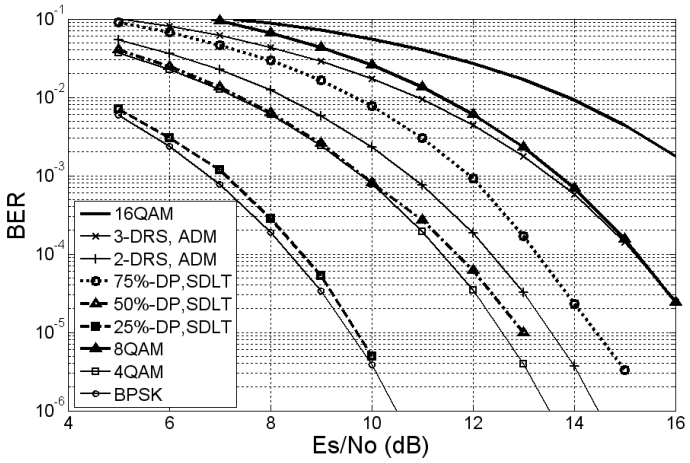

Fig. 10. BER performance of different scheme (uncoded)

5.2 Simulation Result with the Raptor Codes

To ensure that both schemes operate at the same condition, all the schemes encode the data using the Raptor code with the same parameters. The m-bits packet is first encoded with a rate-0.95 right regular low-density parity-check (LDPC) codes and m=10000. The resulting block is then encoded with LT codes using the degree distribution presented in [10], and $\varepsilon = 0.16$.

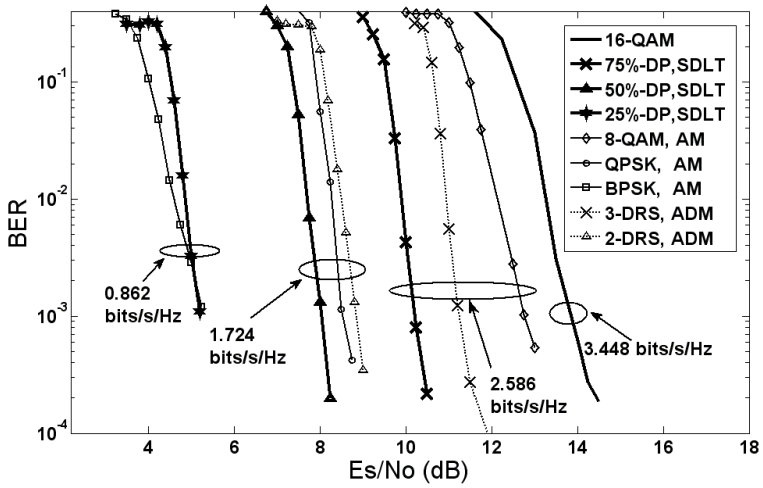

Fig. 11. The BER performance of different schemes with the Raptor codes

The BER performance for these encoded schemes are shown in **Fig. 11**. Simulation results show that our proposed algorithm obtains significant coding gain. Compare with the ADM scheme, simulation results show that SDLT obtains significant coding gain. The SNR gain

between 75%-DP and 3DRS is 1.8 db, the gain between 50%-DP and 2DRS is 1.7 db, at 10^{-3} BER. Compare with the AM scheme, the SNR gain between 75%-DP and 8QAM is 4.6 db, the gain between 50%-DP and QPSK is 1.17 db, the BER performance of 25%-DP is as same as that of BPSK, at 10^{-3} BER. In other words, SDLT outperforms the AM in term of BER performance, when SNR is greater than 5.1 db. Actually, SDLT can work at any $h-DP$ state, since the LLR threshold can flexibility control h. As a result, our scheme have better throughput and adaptability than AM and ADM. Furthermore, if the parameters of the Raptor code can be optimized for a particular demodulation rate h, we would expect to achieve a better performance than the ones shown here.

6. Conclusion

We proposed a new selective demodulation scheme that takes LLR threshold as a key parameter to adjust the rate at the receiver. The proposed scheme outperforms the ADM at BER performance, by using the same algorithms on encoding and decoding. Another main contribution is that it supports much more transmission rate patterns in a large range of channel states, which is very important for the rate adaptive system. We compare the SDLT scheme with the AM scheme, the results also indicate that SDLT can be an effective alternative to the traditional adaptive systems without requiring CSI at the transmitter. In particular, our scheme can work with existing rateless coding and modulation techniques, and requires no changes to them. We are currently working to extend the result to encompass fading channels.

References

[1] Jahon Koo and Kwangsue Chung, "A Mobile-aware Adaptive Rate Control Scheme for Improving the User Perceived QoS of Multimedia Streaming Services in Wireless Broadband Networks," *KSII Transactions on Internet and Information Systems*, vol. 4, no. 6, pp. 1152-1168, Dec, 2010. Article (CrossRef Link)

[2] J. Goldsmith and S. Chua, "Variable-rate variable-power MQAM for fading channels," *IEEE Transactions on Communication*, vol. 45, no. 10, pp. 1218-1230, Oct, 1997. Article (CrossRef Link)

[3] L. Toni, "Does Fast Adaptive Modulation Always Outperform Slow Adaptive modulation," *IEEE Transactions on Wireless Communications*, vol 10, no. 5, pp. 1504-1513, May, 2011. Article (CrossRef Link)

[4] H. Bischi, H. Brandt and T. Cola, "Adaptive coding and modulation for satellite broadband networks: theory and practice," *Wiley Int. J. Satell. Commun. Netw*, vol. 28, no. 2, pp. 59-111, April, 2010. Article (CrossRef Link)

[5] A. Ljaz, A. Awosyila and B. Evans, "Signal-to-noise ratio estimation algorithm for adaptive coding and modulation in advanced digital video broadcasting-radar cross section satellite systems," *IET Communications*, vol. 6, no. 11, pp. 1587-1593, July, 2012. Article (CrossRef Link)

[6] S. Sesia, G. Caire, and G. Vivier, "Incremental redundancy Hybrid ARQ schemes based on low-density parity-check codes," *IEEE Transactions on Communication*, vol. 52, no. 8, pp. 1311-1321, Aug, 2004. Article (CrossRef Link)

[7] Sangjoon Park and Younghoon Whang, "Extended Detection for MIMO Systems with Partial Incremental Redundancy Based Hybrid ARQ," *IEEE Transactions on Wireless Communications*, vol 11, no. 10, pp. 3714-3722, Oct, 2012. Article (CrossRef Link)

[8] S. Q. Hu, Y. D. Yao and A. U. Sheikh, "Tagged user approach for finite-user finite-buffer S-Aloha analysis in AWGN and frequency selective fading channels," in *Proc. of 34th IEEE Sarnoff Symposium*, pp. 1-5, May, 2011. Article (CrossRef Link)

[9] Y. H. Huang, Y. Dong and Y. Z. Liu, "A New Rate Adaptive System: Controlled Solf Demodulation," in *Proc. of IEEE Computing Communications and Applications. HongKong, China*, pp. 360-364, Jan, 2012. Article (CrossRef Link)

[10] J. D. Brown, S. Pasupathy and K. N. Plataniotis, "Adaptive demodulation using rateless erasure codes," *IEEE Transactions on Communication*, vol. 54, no. 9, Sep, 2006. Article (CrossRef Link)

[11] J. D. Brown, J. Abouei and K. N. Plataniotis, "Adaptive demodulation in differentially coherent phase systems: Design and performance analysis," *IEEE Transactions on Communication*, vol. 59, pp. 1772-1778, May, 2011. Article (CrossRef Link)

[12] M. Luby, "LT codes," in *Proc. of 43rd Symp. Found. Comput. Sci., Vancouver, BC, Canada*, pp. 271-282, Nov, 2002. Article (CrossRef Link)

[13] A. Shokrollahi, "Raptor codes," *IEEE Trans .Inf. Theory*, vol. 52, no. 6, pp. 2551-2567. June, 2006. Article (CrossRef Link)

[14] Y. J. Fan and L. F. Lai, "Rateless coding for MIMO fading channels: Performance limits and code construction," *IEEE Trans. Wireless Commun*, vol. 9, no. 4, pp. 1288-1292, April, 2010. Article (CrossRef Link)

[15] Sivasubramanian and H. Leib, "Fixed-rate raptor codes over Rician fading channels," *IEEE Trans. Veh. Technol*, vol. 57, no. 6, pp. 3905-3911, Nov, 2008. Article (CrossRef Link)

[16] Hagh, M. J and Soleymani, "Application of Raptor Coding With Power Adaptation to DVB Multiple Access Channels," *IEEE Trans. Broadcasting*, vol. 58, no. 3, pp. 379-389, Sep, 2012. Article (CrossRef Link)

[17] S. Y. Legoff, "Signal constellations for bit-interleaved coded modulation," *IEEE Trans. Inf. Theory*, vol. 49, no. 1, pp. 307-313, Jan, 2003. Article (CrossRef Link)

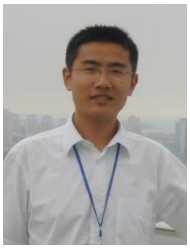

Yuheng Huang received the B.S. degree from Haerbin Engineering University, Haerbin, China, in 2005 and M.S. degree from Huazhong University of Science & Technology, Wu Han, China, in 2008. He is currently a Ph.D. candidate in department of Electronics and Information Engineering, Huazhong University of Science &Technology. His research interests include Wireless Sensor Network, compressed Sensing and Channel Coding.

Yan Dong is a associate professor of Huazhong University of Sci.&Tech, WuHan, China. Her main research field is broadband wireless communication and Space Communication Networks. From 2000 to 2001, he was a postdoctoral researcher in Paris University XI

Minho Jo received his Ph.D. degree from the Department of Industrial and Systems Engineering, Lehigh University, Pennsylvania, in 1994. He was a staff researcher with Samsung Electronics. He is currently a Brain Korea Professor at Korea University, Seoul.

Yingzhuang Liu is a professor of Huazhong University of Sci.&Tech, WuHan, China. His main research field is broadband wireless communication, including LTE and IMT Advanced system, etc., especially its Radio Resource Management. From 2000 to 2001, he was a postdoctoral researcher in Paris University XI.